Kinetics and thermodynamics of adsorption of red dye 40 from acidic aqueous solutions onto a novel chitosan sulfate

N. Rios-Donato[a], A.M. Peña-Flores[a], I. Katime[b], R. Leyva-Ramos[c] and E. Mendizábal[a]*

[a]Departamento de Química, Universidad de Guadalajara, M. García Barragán 1451, Guadalajara, Jalisco 44430, México. [b]Grupo de Nuevos Materiales y Espectroscopia Supramolecular. Campus de Leioa, Universidad del País Vasco. Vizcaya. España. [c]Centro de Investigacion y Estudios de Posgrado, Facultad de Ciencias Quimicas, Universidad Autonoma de San Luis Potosi, Av. Dr. M. Nava No. 6, San Luis Potosi SLP 78210, Mexico

Cinética y termodinámica de la adsorción del colorante rojo 40 de disoluciones acuosas ácidas utilizando un novedoso sulfato de quitosano

Cinètica i termodinàmica de l'adsorció del colorant vermell 40 de dissolucions aquoses àcides utilitzant un nou sulfat de quitosà

RECEIVED: 22 SEPTEMBER 2016; REVISED: 25 NOVEMBER 2016; ACCEPTED 13 DECEMBER 2016

SUMMARY

The kinetic and thermodynamics of adsorption of Red Dye 40 from acidic aqueous solutions onto a partially sulfated chitosan (ChS) was studied. The partially sulfated ChS was water insoluble in the pH range of 2-12. Experiments were carried out batch-wise to determine the effect of pH, dye concentration, and temperature on the adsorption capacity of ChS towards Red Dye 40. It was found that the equilibrium dye-binding capacity of ChS (q_e) increased with increasing initial dye concentration; however, the percentage of dye removal decreased. Dye adsorption capacity of ChS increased when the solution pH was reduced. The Langmuir model was better fitted the experimental adsorption equilibrium data, and the rate of dye adsorption onto ChS follows the pseudo-second order kinetic model. The adsorption capacity of ChS was enhanced by increasing the temperature. The thermodynamic adsorption parameters, enthalpy (ΔH°), entropy (ΔS°), and Gibbs energy (ΔG°) were evaluated. The adsorption process was endothermic, and the Gibbs energy negative indicating that it occurred spontaneously.

Keywords: Adsorption; chitosan sulfate; pH; Red Dye 40.

RESUMEN

Se estudió la cinética y la termodinámica de la adsorción de Red Dye 40 de soluciones acuosas ácidas utilizando un quitosano parcialmente sulfatado (ChS). El ChS parcialmente sulfatado era insoluble en agua en el intervalo de pH de 2 - 12. Los experimentos se llevaron a cabo por lotes para determinar el efecto del pH, la concentración de colorante y la temperatura en la capacidad de adsorción del ChS de Colorante Rojo 40. Se encontró que la capacidad de adsorción de colorante en el equilibrio por el ChS (q_e) se incrementaba con el aumento de la concentración inicial del colorante; sin embargo, el porcentaje de eliminación de colorante disminuía. La capacidad de adsorción del colorante por el ChS aumentó cuando se redujo el pH de la disolución. El modelo de Langmuir fue el que mejor se ajustó a los datos experimentales de adsorción en el equilibrio y la cinética de adsorción del colorante siguió un modelo cinético de pseudo-segundo orden. La capacidad de adsorción de ChS se mejoró aumentando la temperatura. Se evaluaron los parámetros termodinámicos de adsorción, entalpía (ΔH °), entropía (ΔS °) y energía libre de Gibbs (ΔG °). El proceso de adsorción fue endotérmico y la energía libre de Gibbs negativa indicando que el proceso ocurrió de manera espontánea.

Palabras clave: Adsorción; sulfato de quitosano; pH; colorante rojo 40.

RESUM

Ls va estudiar la cinètica i la termodinàmica de l'adsorció de Red Dye 40 de solucions aquoses àcides fent servir un quitosà parcialment sulfatat (ChS). El ChS parcialment sulfatat era insoluble en aigua en l'inter-

***Corresponding author: lalomendizabal@hotmail.com**

val de pH de 2 - 12. Els experiments es van dur a terme per lots per determinar l'efecte del pH, la concentració de colorant i la temperatura en la capacitat d'adsorció del ChS de Colorant Vermell 40. Es va trobar que la capacitat d'adsorció de colorant en l'equilibri pel ChS (q_e) s'incrementava amb l'augment de la concentració inicial del colorant; però, el percentatge d'eliminació de colorant disminuïa. La capacitat d'adsorció del colorant pel ChS va augmentar quan es va reduir el pH de la dissolució. El model de Langmuir va ser el que millor es va ajustar a les dades experimentals d'adsorció en l'equilibri i la cinètica d'adsorció del colorant va seguir un model cinètic de pseudo-segon ordre. La capacitat d'adsorció de ChS va millorar augmentant la temperatura. Es van avaluar els paràmetres termodinàmics d'adsorció, entalpia (ΔH °), entropia (ΔS °) i energia lliure de Gibbs (AG °). El procés d'adsorció va ser endotèrmic i l'energia lliure de Gibbs negativa indicant que el procés tenia lloc de manera espontània.

Paraules clau: Adsorció; sulfat de quitosà; pH; colorant vermell 40.

INTRODUCTION

At present, wastewater discharge from dyeing industries (textiles, leather, dyestuff, paper, plastics, etc.) is a major concern for the environment because they release large volumes of polluted wastewater containing dyes[1,2] Textile effluents usually contain slight amounts of dyes that, nevertheless, give color to the water[3]. The treatment of these wastewaters has been for many years the subject of study. Azo dyes are very soluble in water, highly resistant to the action of chemical agents, have low biodegradability, affect biological activity of water and allow only limited light penetration. Different treatments and combinations thereof have been tested for removal of dyes from wastewater: chemical coagulation, biological treatment, Fenton, electrochemical oxidation, ozonation, ultrafiltration, photocatalysis, adsorption and electrocoagulation[4,5.] Adsorption, which is a widely used method for its simple design, easy operation and flexibility, is an effective method for dye removal[1]. The uptake of a dye by an adsorbent from a water solution depends on process variables such as adsorbent type, particle size and dosage, initial dye concentration, contact time, agitation speed, pH, and temperature[6]. Several adsorbents have been tested for the removal of dyes (activated carbon, swede rape straw *"Brassica napus L."*, babassu palm, chitin, hydrilla verticillata, silica, etc.)[7–9]. Among these adsorbents, chitosan is currently one of the most studied because of its abundance, biodegradability, low-cost and good removal capacity[10].

Chitosan (Ch) has three types of reactive functional groups, an amino group and two hydroxyl groups (primary and secondary) at the C-2, C-3 and C-6 positions, respectively. Its chemical structure allows specific modifications relatively easy, especially, at the C-2 position. However, because the amino groups of Ch are protonated as pH decreases, the Ch becomes water-soluble. At a pH value near 3.0, the amino groups are completely protonated[11]; consequently, Ch cannot be applied for the removal of dyes from aqueous solutions with acidic pH[1]. Chitosan has been modified to enhance its acid and mechanical resistance in aqueous solution. The modification has been carried out by several routes such as crosslinking reaction with epichlorohydrin, ethylene glycol, 1,4-butanediol diglycidyl ether or glutaraldehyde and chemical modifications1[2,13], however, in some cases the amount of amino groups, which are the primary sites responsible for dye adsorption, are lessened during the modification[1]. Recently, Rios-Donato et al[14] reported a method for synthesizing chitosan sulfate (ChS) with a partial degree of sulfation, with an insolubility window between pH 5.0 and 8.0 without modifying the amino groups. Furthermore, ChS insoluble in a range of pH´s of 2 to 12 was prepared using a slightly modified synthesis method and showed to have a good capacity for dyes removal from dilute solutions (20 mg/L)[15].

In this work, a partially sulfated chitosan (ChS) water-insoluble at pH´s from 2 to 12 was synthesized and used to remove Red Dye 40 from acidic aqueous solutions. Moreover, the adsorption of the Red Dye 40 on ChS was studied in a batch adsorber. The capacity of the ChS for adsorbing the Red dye 40 from aqueous solutions was studied as a function of pH, dye concentration, and temperature, and the thermodynamic adsorption parameters were evaluated. In addition, the order of the adsorption kinetics was obtained.

EXPERIMENTAL

Chitosan food grade (Ch) with a degree of deacetylation of 90% was from América Alimentos S.A de C.V. Acetic acid (Fermont), Dimethylformamide, DMF (Flucka), Chlorosulfonic acid (Sigma-Aldrich) and methanol (Fermont) were used as received. Red Allure E-123 (Red Dye 40) was used as received, and its chemical structure is displayed in Figure 1. All solutions were prepared using double distilled water.

ChS was synthesized using a modification of the method proposed by Rios et al[14]. Ch was dissolved in acetic acid aqueous solution (0.12 M) and precipitated by adding a NaOH aqueous solution (0.25 M). The suspension was filtered, and the precipitate was washed with water until neutral pH and then with methanol. The precipitate was soaked in DMF and stirred for 30 min to eliminate the methanol, and the liquid was separated by decantation. This procedure was repeated until complete removal of the methanol. The precipitate was kept soaked in DMF. Soon afterward, chlorosulfonic acid was added dropwise to DFM keeping the temperature at 0°C to produce the salt $HClSO_3$-DMF. Then, the salt was dissolved in toluene, added to the mixture of chitosan-DMF and stirred for 2 hours to obtain the ChS. The ChS was separated by decantation, washed with methanol, soaked in distilled water, and the pH was adjusted to 7.0 by adding an aqueous solution of NaOH 0.1 N. The ChS was subsequently purified using a cellulose dialysis membrane with a

MWCO of 12,000 g mol^{-1} (Sigma, Aldrich) until the addition of a solution of $BaCl_2$ to the dialyzed water did not show a precipitate. Once purified, the ChS was dried at 45 °C and then ground in an agate mortar to obtain particle sizes ranging from 62 to 149 microns.

The Fourier transform infrared spectra (FTIR) of the ChS was obtained in an FTIR spectrometer, Perkin–Elmer (Model Spectrum 100). The dried sample was mixed with reagent-grade KBr in a ChS/KBr ratio of 1/10, and the sample was mechanically pressed to obtain a pellet. The sulfur/nitrogen (S/N) ratio was quantified in an Elemental Analyzer, Leco TruSpec Micro Series (Missouri, USA). Sulfamethazine (Leco, Missouri, USA) was used as the standard reference. The analysis was carried out in triplicate.

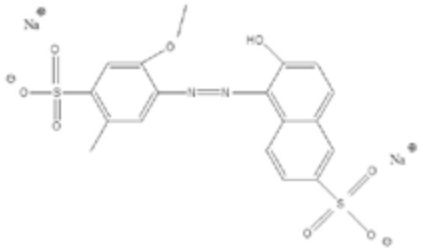

Figure 1. *Chemical structure of the Red Dye 40.*

Aqueous solutions with concentrations of Red Dye 40 in the range between 20 and 4500 mgL^{-1} were prepared and the solution pH was adjusted to 3.0 or 6.0 using 0.1 M HCl and 0.1 M NaOH solutions. A volume of 10 mL of the dye solution and 0.01 g of ChS were added to a centrifuge vial, which acted as the batch adsorber. The batch adsorbers were placed in a Thermo Scientific precision reciprocal shaking water bath and maintained at 25°C under continuous agitation (200 rpm) until reaching equilibrium. The particles were separated from the dye solution by centrifugation for 3 minutes at 2500 rpm (Centrifuge Unico C8706). The concentration of the residual dye in the water solution (Ct) was determined using a UV-visible spectrophotometer at the wavelength of 500 nm. The amount of dye adsorbed by unit of weight (q_e) was

$$q_e = \frac{(C_0 - C_e)V}{m} \qquad (1)$$

where C_0 is the initial concentration of dye (mg mL^{-1}), C_e is the concentration of dye at equilibrium (mg mL^{-1}), V is the volume of the dye solution (10 mL), and *m* is the mass of ChS (g). Each run was carried out in triplicate, and the average result was reported. The effect of temperature on the adsorption capacity was studied by performing adsorption experiments at dye concentrations from 50 to 3000 mg/L, temperatures of 25, 35, 45 and 55 °C, and pH = 3.0.

Experiments were carried out to study the rate of adsorption at pH = 3.0 and T = 25 °C. The procedure for obtaining the curves of the amount of dye adsorbed vs. time was very similar to that for adsorption equilibrium. In this case, the centrifuge vials containing 10 mL of the dye aqueous solution and 0.01 g of ChS were placed in the shaking water bath. At predetermined time intervals, a vial was removed from the water bath and centrifuged to separate the ChS particles from the solution. The solution was analyzed to determine the concentration of the dye at a given time, C_t. The mass of dye adsorbed at time t, q_t, was calculated by equation (1) using C_t instead of C_e.

RESULTS AND DISCUSSION

The ChS is an amber solid, water-insoluble in the pH range of 2-12 and has a molecular weight greater than 12,000 g/mol, which is the pore size of the dialysis membrane used in the purification. Elemental analysis revealed that the S/N ratio was 0.47.

Figure 2a shows the characteristic bands of Ch, a broad peak at around 3430 cm^{-1} due to the OH and amino groups, the peak of the carbonyl group at 1640 cm^{-1} and the pyranose ring signal at 1070 cm^{-1}; [16,17]; all the peaks are consistent with those reported for the Ch[18]. ChS spectrum (Figure 2b) shows, in addition to these peaks, stretch peaks of C-O-S (800 cm^{-1}) and S=O (1250 cm^{-1}) confirming that the ChS was obtained.

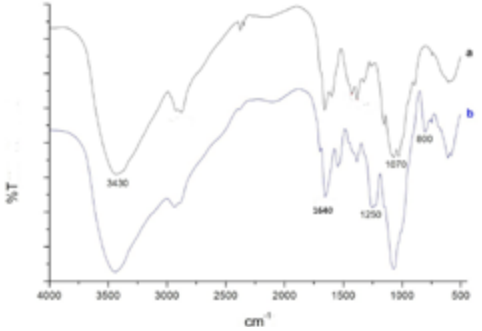

Figure 2. *FTIR spectra of Ch (a) and ChS (b).*

The chemical structure of the ChS is illustrated in Figure 3.

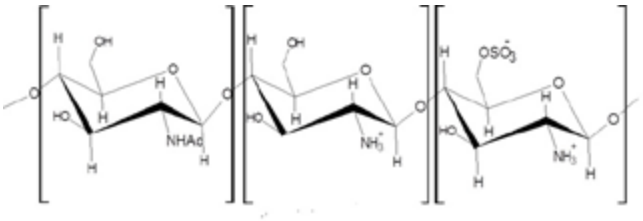

Figure 3. *Chemical structure of the monomeric units of ChS.*

The adsorption equilibrium data were interpreted using the Langmuir and Freundlich isotherms. The Langmuir isotherm model is based on the assumption that the surface is energetically homogeneous; i.e., all adsorption sites are the same[19]. This isotherm can be mathematically represented in the linear form as follows:

$$\frac{C_e}{q_e} = \frac{C_e}{q_m} + \frac{1}{K_L q_m} \qquad (2)$$

where C_e is the concentration of dye at equilibrium (mg L^{-1}), K_L is the Langmuir constant related to the affinity of binding sites (L g^{-1}), q_e is the amount of dye adsorbed at equilibrium (mg g^{-1}) and q_m is the maxi-

mum adsorption capacity of ChS (mg g^{-1}). A straight line is obtained by plotting C_e/q_e versus C_e, and the slope and y-intercept of this straight line are $1/q_m$ and $1/(K_L q_m)$, respectively.

The Freundlich adsorption isotherm is an empirical model and can be linearized as follows:

$$\log q_e = \log K_F + \frac{1}{n}\log C_e \qquad (3)$$

where K_F is the Freundlich isotherm constant related to the adsorption capacity ($mg^{1-1/n}\ L^{1/n}\ g^{-1}$) and *n* is the intensity of adsorption. The plot of log q_e versus log C_e results in a straight line with a slope of 1/n and the y-intercept is log K_F.

The Langmuir and Freundlich models were fitted to the experimental adsorption equilibrium data and the linear graphs for both models are shown in Figure 4, and the parameters for both isotherm models are given in Table 1. Figure 4 and Table 1 show that the Langmuir model provides a much better fit than the Freundlich model. The experimental adsorption isotherms are fairly well reproduced by the Langmuir model at both pH´s (Figure 5).

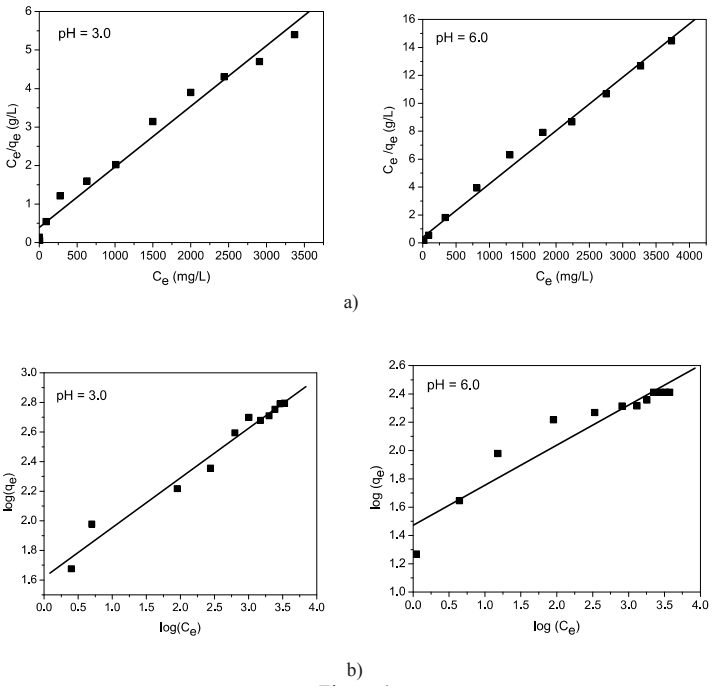

Figure 4. *Linear plots of the adsorption isotherms of Red Dye 40 onto ChS at T = 25 ^{0}C. a) Langmuir, b) Freundlich.*

Table 1. *Isotherm constants of the Langmuir and Freundlich models for adsorption of Red Dye 40.*

T (°C)	pH	Freundlich			Langmuir		
		K_F ($mg^{1-1/n}\ L^{1/n}$ /g	n	R^2	q_m (mg/g)	K_L (L/mg)	R^2
25	3.0	40.0	2.9	0.972	623	$4.0x10^{-3}$	0.976
25	6.0	29.5	3.55	0.908	261	$3.7x10^{-3}$	0.976
35		50.0	2.9	0.947	613	$14x10^{-3}$	0.984
45	3.0	18.1	1.94	0.881	840	$17x10^{-3}$	0.986
55		26.9	2.05	0.970	892	$26x10^{-3}$	0.996

Figure 5 shows the adsorption of the Red Dye 40 onto ChS at 25 ^{0}C and pH of 3.0 and 6.0. At pH 3.0, the equilibrium dye-binding capacity (q_e) increased with increasing initial dye concentration (C_0) and levels off at around q_e = 623 mg g^{-1}. The q_e increase is due to the larger dye concentration gradient obtained when using higher initial dye concentration (C_0). However, the percentage of removal decreased when increasing C_0 (94.4% at C_0 = 20 mg L^{-1} to 15.5% at C_0 = 4000 mg L^{-1}). At low dye concentrations the ratio of dye molecules to the available adsorption sites is small, so that the percentage of removal is high, whereas at high dye concentrations, the ratio becomes larger, and the percentage of removal is reduced[1]. A quick calculation considering that ChS has an average molecular weight of the monomeric unit of 211 and a degree of deacetylation of 90%, it is obtained that at q_e = 623 mg g^{-1} (maximum adsorption) about 27% of the amino groups were used to adsorb the dye. However, some protonated OH groups can also participate in the adsorption of the dye.

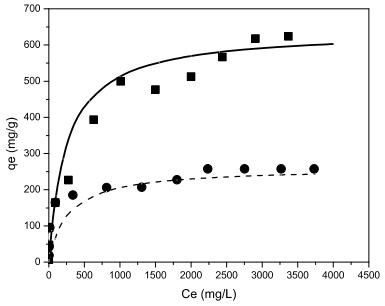

Figure 5. *Adsorption of Red Dye 40 onto ChS at 25 ^{0}C. pH=3.0, experimental (■), Langmuir (▬▬); pH=6.0, experimental (●), Langmuir (- -).*

Figure 5 shows that raising the pH from 3 to 6 considerably decreased the adsorption capacity of ChS. The shape of both curves indicates that the isotherms are L-class. At T = 25 °C, the maximum adsorption capacities of ChS, q_m, were 623 and 261 mg g^{-1} at pH = 3 and pH = 6.0, respectively. These values indicate that the adsorption capacity decreased around 58 % when the pH was raised from 3 to 6. Pietrelli et al[2]. reported smaller dye adsorption capacities when using chitosan to remove several types of dyes at pH 6.

The chemical structure of Red Dye 40 (Figure 1) reveals that it is an anionic dye because of its sulfate groups. The effect of the pH on the adsorption capacity of ChS towards Red Dye 40 can be attributed to the electrostatic interactions between the protonated amine groups of ChS and the sulfate groups of the dye. The adsorption capacity of ChS was decreased when the pH was raised from 3 to 6 since the concentration of protonated amino groups on the surface of ChS was decreased, resulting in that less dye molecules can be adsorbed by electrostatic interactions(Rios-Donato et al. 2012).

The protonation of amino group is described by the following reaction:

$\equiv CH\text{-}NH_2 + H^+ \rightarrow \equiv CH\text{-}NH_3^+$

where ≡CH represents the surface of the chitosan.

The electrostatic attraction between the dye molecule and the surface of ChS can be represented by the following reaction:

$\equiv CH\text{-}NH_3^+ + Dye\text{-}SO_4^- \rightarrow \equiv CH\text{-}NH_3^+Dye\text{-}SO_4^-$

where $Dye\text{-}SO_4^-$ represents the Red Dye 40.

The dependence of adsorption capacity on temperature was studied by carrying out adsorption equilibrium experiments at different initial dye concentrations (50, 100, 1000, 2000 y 3000 mg L^{-1}) and the temperatures of 25, 35, 45 and 55°C. Figure 6 shows that the amount of Red Dye 40 adsorbed increased when the temperature was augmented.

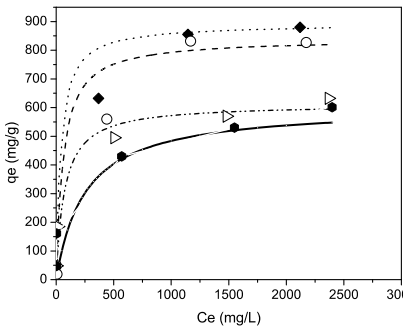

Figure 6. *Effect of temperature on the adsorption isotherms of Red Dye 40. Symbols represent experimental data and lines are the prediction of the Langmuir model: 25 °C(●)(▬▬), 35 °C(▷)(▬ ▪ ▬), 45 °C(○)(▬ ▬), 55 °C (◆) (▬ ▪ ▪ ▬)*

For very low concentrations of dye at equilibrium, the effect of temperature is very slight, whereas, for high concentrations of dye at equilibrium, there is a significant increase in the adsorption capacity. For example, at an initial dye concentration of 2000 mg L^{-1}, the adsorption capacity of ChS was 554, 582, 816 and 875 mg g^{-1} at the temperatures of 25, 35, 45 y 55 °C, respectively. In other words, the adsorption capacity was augmented around 1.6 times when the temperature was increased from 25 to 55 °C.

It has been reported that the uptake of dyes adsorbed on chitosan increased with temperature[16,17,20,21]. If the solution temperature is raised there are a greater number of active sites[22] temperature, and more dye molecules in the solution have enough energy to become adsorbed on the surface of ChS[21,23].

The adsorption thermodynamic parameters are necessary for a better understanding of the adsorption process. The thermodynamic parameters, enthalpy (ΔH°), entropy (ΔS°), and Gibbs energy (ΔG°) of dye adsorption on ChS can be calculated from the following equations:

$$\Delta G^0 = -RT\ln K \qquad (4)$$

$$\Delta G^0 = \Delta H^0 - T\,\Delta S^0 \qquad (5)$$

where R is the universal gas constant, T is the absolute temperature and K is the equilibrium constant. Combining equations (4) and (5), the following linear relationship between K and 1/T results:

$$\ln K = -\frac{\Delta H^0}{RT} + \frac{\Delta S^0}{R} \qquad (6)$$

The equilibrium constant (K) can be obtained from different adsorption isotherm equations (Langmuir, Flory-Huggins, Frumkin isotherms) or distribution constants, (q_e/C_e, C_{ad}/C_e)[24] .The values of equilibrium constant will vary depending on the calculation method, resulting in poor estimates of ΔH°, ΔS°, and ΔG°. For neutral or with very weak charge adsorbates, it is recommended to use the Langmuir equilibrium constant, K_L (L/mol), as the thermodynamic equilibrium adsorption constant[24]. Figure 7 shows the plot of ln K_L versus 1/T, where the values of ΔH° and ΔS° were obtained from the slope and y-intercept respectively. Langmuir isotherm constants and thermodynamic parameters are listed in Table 2. The positive value of ΔH° indicates that adsorption of the dye on CHS is endothermic. The value of ΔH° was greater than 42 kJ mol^{-1}, indicating that the interaction between dye and surface of ChS is strong[25]. In other words, the Red Dye 40 was chemically adsorbed on the ChS surface. Unlike gas adsorption, where only one process is considered, gas adsorbed onto the solid; in liquids adsorption there are two processes: displacement of the water molecules from the active sites which require energy, followed by the adsorption of the adsorbate molecules that results in release of energy, the energy balance being that the process is endothermic[26].

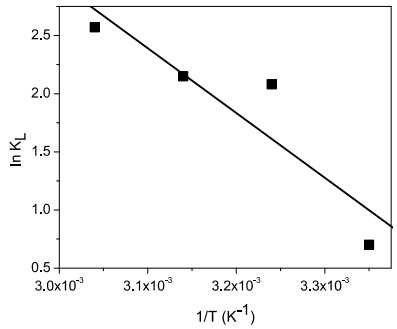

Figure 7. *Ln K_L versus 1/T.*

The Gibbs energy, ΔG°, is negative and increased with temperature, (Table 2) indicating that the adsorption process is favorable for the adsorption of Red Dye 40 onto ChS.

Table 2. *Thermodynamic parameters for the adsorption of Red Dye 40 onto ChS.*

Temperature (°C)	K_L (L/mol)	ΔG° (kJ/mol)	ΔH° (kJ/mol)	ΔS° (kJ/mol °K)
25	1.98	-2.09		
35	6.60	-3.62	43.5	0.153
45	7.79	-5.15		
55	11.13	-6.68		

Adsorption kinetics was studied at T = 25 °C, pH = 3.0 and initial dye concentrations of 50, 100, and 200 mgL^{-1}. Figure 8 shows that the equilibrium adsorption capacity (q_e) increased by raising the initial concentration of dye. The time to attain equilibrium was about 240 minutes for all initial concentrations.

The pseudo-first-order and pseudo-second order kinetic models were fitted to the experimental adsorption kinetic data, to determine the adsorption

rate mechanism of dye. According to Langergren[17] the pseudo-first-order kinetic model is given by the subsequent equation:

$$\log(q_e - q_t) = \log(q_e) - k_1 t \quad (7)$$

where q_t is the mass of dye adsorbed at time *t*, and k_1 is the first order rate constant. By plotting $\log(q_e - q_t)$ versus t, a straight line should be obtained with a slope of $-k_1$ and y-intercept of $\log(q_e)$.

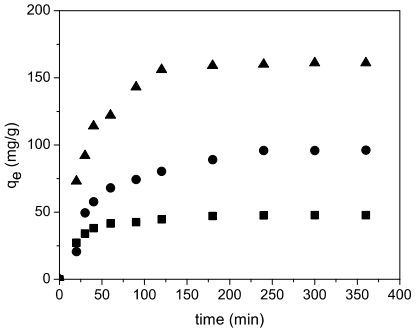

Figure 8. *Adsorption kinetics of Red Dye 40 at pH = 3.0, T = 25 °C, and initial dye concentrations of 50 (■),100 ((●), (▲) 200 mg L^{-1}.*

The pseudo-second-order kinetic equation [27] is:

$$\frac{t}{q_t} = \frac{1}{k_2 q_e^2} + \frac{1}{q_e} t \quad (8)$$

where k_2 is the second order rate constant. The plot of t/q_t versus t should give a straight line with a slope of $1/q_e$ and y-intercept of $1/(k_2 q_e^2)$. The initial adsorption rate (h_0) can be estimated when t = 0 and is given by:

$$h_0 = k_2 q_e^2 \quad (9)$$

Table 3 shows the kinetic parameters obtained by fitting the first and second-order kinetic models to the experimental data.

Table 3. *Parameters of the kinetic models for the adsorption of dye onto ChS.*

Pseudo-first-order					*Pseudo-second-order*			
C_0 mg/L	$q_{e,exp}$ mg/g	$q_{e,cal}$ mg/g	$k_1 x10^3$ 1/min	R^2	$q_{e,cal}$ mg/g	$k_2 x10^4$ g/(min mg)	h_0 mg/(g min)	R^2
50	47.7	27.8	8.9	0.985	49.9	14.7	3.66	0.999
100	95.9	74.1	5.8	0.963	111.8	3.79	4.03	0.983
200	161	101.5	2.0	0.950	210	2.17	9.6	0.998

At all initial dye concentrations used, the correlation coefficients (R^2) are closer to 1.0 and the calculated q_e values, are much nearer to the experimental data for the pseudo-second-order model than those for the pseudo-first-order model. Then, Red Dye 40 adsorption onto ChS follows the pseudo-second-order kinetic model indicating that the rate-limiting step may chemisorption by sharing or exchange of electrons between sorbent and sorbate[27]. Table 3 also indicates that k_2 decreases by reducing the initial concentration of dye, and because the larger driving force, the initial adsorption rate (h_0) increases as the initial dye concentration augments. Similar behavior on the adsorption of a dye onto a chitosan/zeolite biocomposite has been reported elsewhere[21].

CONCLUSIONS

Because chitosan can not be used at low pH´s, the ChS synthetized is a good alternative to remove Red dye 40 from acidic aqueous solutions. ChS has larger dye adsorption capacity than that reported for Ch. Dye adsorption capacity of ChS increased when the solution pH was reduced from 6 to 3. Raising the initial concentration of dye increased the uptake of dye adsorbed; however, the percentage of dye removal decreased. The Langmuir model better fitted the experimental adsorption equilibrium data. Increasing the temperature resulted in a larger ChS adsorption capacity. The positive value of ΔH° indicates that adsorption of the dye on ChS is an endothermic process. The adsorption of Red Dye 40 onto ChS follows the pseudo-second-order kinetic model.

ACKNOWLEDGMENTS

This research was supported by a grant from the Mexican Council of Science and Technology, CONACYT, (CB-2014-1-241108).

REFERENCES

1. Crini, G. ; Badot, P.-M. Application of chitosan, a natural aminopolysaccharide, for dye removal from aqueous solutions by adsorption processes using batch studies: A review of recent literature. *Prog. Polym. Sci.* **2008**, *33*, 399–447.
2. Pietrelli, L.; Francolini, I.; Piozzi, A. Dyes Adsorption from Aqueous Solutions by Chitosan. *Sep. Sci. Technol.* **2015**, *50*, 1101–1107.
3. No, H.K.; Meyers, S.P. Handbook of carbohydrate Engineering, **2005**,*2*, 535-562.
4. Shawaqfah, M.; Momani, F.A.Al.; Al-anber, Z.A. Ozone Treatment of Aqueous Solutions Containing Commercial Dyes. *Afinidad,* ***2012****, 69,* 229–234.
5. Neto, B.; Lins, V. Black B dye by Fenton and photo-Fenton. *Afinidad*, **2009**, *66*, 232–237.
6. Vaghela, S.S. *et al.* Laboratory Studies of Electrochemical Treatment of Industrial Azo Dye Effluent. *Environ. Sci. Technol.* **2005**, *39*, 2848–2855.
7. Blackburn, R.S. Natural Polysaccharides and Their Interactions with Dye Molecules: Applications in Effluent Treatment †. *Environ. Sci. Technol.****2004****, 38*, 4905–4909.
8. Rajesh Kannan, R.; Rajasimman, M.; Rajamohan, N. ; Sivaprakash, B. Equilibrium and kinetic studies on sorption of malachite green using Hydrilla Verticillata biomass. *Int. J. Environ. Res.***2010**, *4*, 817–824 .
9. Robinson, T.; McMullan, G.; Marchant, R.; Nigam, P. Remediation of dyes in textile effluent: A critical

review on current treatment technologies with a proposed alternative. *Bioresour. Technol.**2001**, 77,* 247–255 .
10. Saha, T. K.; Karmaker, S.; Ichikawa, H.; Fukumori, Y. Mechanisms and kinetics of trisodium 2-hydroxy-1,1'-azonaphthalene-3,4',6-trisulfonate adsorption onto chitosan. *J. Colloid Interface Sci.* **2005**, *286*, 433–439.
11. Chen, A.-H.; Huang, Y.-Y. Adsorption of Remazol Black 5 from aqueous solution by the templated crosslinked-chitosans. *J. Hazard. Mater.**2010**, 177,* 668–75.
12. Gong, R.; Li, N.;Cai, W.; Liu, Y.; Jiang, J. α-Ketoglutaric Acid-Modified Chitosan Resin As Sorbent for Enhancing Methylene Blue Removal From Aqueous Solutions. *Int. J. Environ. Res.* **2012**, *4,* 27–32.
13. Rinaudo, M. Chitin and chitosan: Properties and applications. *Prog. Polym. Sci.* **2006**, *31,* 603–632.
14. Rios-Donato, N.; Navarro, R.; Avila-rodriguez, M.; Mendizabal, E. Coagulation – Flocculation of Colloidal Suspensions of Kaolinite , Bentonite , and Alumina by Chitosan Sulfate. *J. Appl. Polym. Sci.* **2012**, *123,* 2003–2010.
15. Ríos-Donato, N.; Marmolejo-Carranza, R.; García, R.; Blanco-Aquino, A.; García-Gaytán, B. ; Mendízabal, E. Eliminación de colorantes de disoluciones acuosas utilizando sulfato de quitosano. *Rev. Iberoam. Polímeros.* **2013**, *14*, 257–263 (2013).
16. Saha, T. K. Adsorption of Methyl Orange onto Chitosan from Aqueous Solution. *J. Water Resour. Prot.* **2010**, *2*, 898–906.
17. Annadurai, G. Adsorption of basic dye on strongly chelating polymer: Batch kinetics studies. *Iran. Polym. J.* **2002**, *11*, 237–244.
18. Vongchan, P.; Sajomsang, W.; Kasinrerk, W.; Subyen, D. Anticoagulant Activities of the Chitosan Polysulfate Synthesized from Marine Crab Shell by Semi-heterogeneous Conditions. *Symp. A Q. J. Mod. Foreign Lit.* **2003**, 29, 115–120.
19. Chiou, M.-S.; Ho, P.-Y.; Li, H.-Y. Adsorption of anionic dyes in acid solutions using chemically cross-linked chitosan beads. *Dye. Pigment.* **2004**, *60*, 69–84.
20. Cestari, A. R.; Vieira, E.F.S.; Dos Santos, A.G.P., Mota, J.A.; De Almeida, V.P. Adsorption of anionic dyes on chitosan beads. 1. The influence of the chemical structures of dyes and temperature on the adsorption kinetics. *J. Colloid Interface Sci.* **2004**, *280,* 380–386.
21. Metin, A.; Ciftci, H.; Alver, E. Efficient Removal of Acidic Dye Using Low-Cost Biocomposite Beads. *Ind. Eng. Chem. Res.* **2013**, *52*, 10569–10581.
22. Uzun, I. Kinetics of the adsorption of reactive dyes by chitosan. *Dye. Pigment.* **2006**, *70*, 76–83.
23. Srivastava, V.C.; Swamy, M.M.; Mall, I.D.; Prasad, B.; Mishra, I. M. Adsorptive removal of phenol by bagasse fly ash and activated carbon: Equilibrium, kinetics and thermodynamics. *Colloids Surfaces A Physicochem. Eng. Asp.* **2006**, *272*, 89–104.
24. Liu, Y. Is the free energy change of adsorption correctly calculated? *J. Chem. Eng. Data.* **2008**, *54*, 1981–198
25. Froment, G.F.; Bischoff, K.B. *Chemical Reactor Analysis and Design.* John Wiley & Sons, Singapore, 1990.
26. Srivastava, V.C., Mall, I.D.; Mishra, I. M. Adsorption thermodynamics and isosteric heat of adsorption of toxic metal ions onto bagasse fly ash (BFA) and rice husk ash (RHA). *Chem. Eng. J.* **2007**, *132*, 267–278 (2007).
27. Ho, Y.S.; Mckay, G. Pseudo-second order model for sorption processes. *Process Biochem.* **1999**, *34*, 451–465. 5.